DISTRIBUTION STATEMENT A. Approved for public release; distribution is unlimited.

Data Analysis, Modeling, and Ensemble Forecasting to Support NOWCAST and Forecast Activities at the Fallon Naval Station

Darko Koracin
Desert Research Institute
2215 Raggio Parkway
Reno, NV 89512
phone: (775) 674-7091 fax: (775) 674-7016 email: Darko.Koracin@dri.edu

John Lewis
Desert Research Institute
2215 Raggio Parkway
Reno, NV 89512
phone: (775) 674-7077 fax: (775) 674-7016 email: John.Lewis@dri.edu

Grant Number: N00014-08-1-0451
http://www.adim.dri.edu/

LONG-TERM GOALS

The goals of this project are to increase our understanding of weather predictability and its advantages and limitations, and to develop methods to provide more accurate forecasts and nowcasts in complex terrain using multi-model ensemble modeling techniques and special observations including remotely sensed data.

OBJECTIVES

The main objectives of the study are: 1) to further develop, test, and continue twice daily operational forecasts using both the real time Weather and Research Forecasting (WRF Version 3.2) model (Skamarock et al. 2008) and Mesoscale Model 5 (MM5 Version 3.7.2) (Grell et al. 1994) with sub-kilometer horizontal resolution to support the NOWCAST system at the Fallon Naval Air Station (NAS); 2) To extend the real time forecasting system with a continuous 15-day forecast using WRF as a testbed; 3) To analyze multi-model ensemble forecasting capabilities and to provide basis for a real time multi-model ensembles using WRF, MM5, and the Coastal Oceanic and Atmospheric Modeling Prediction System (COAMPS^{TM}, Version 3.1.1) (Hodur 1997); 4) To develop a framework that complements the ensemble forecasting to better understand the sources of error and uncertainty in dynamical forecasts relevant to nowcasting key parameters such as wind speed, cloud fields, and visibility over the Fallon NAS area; and 5) To test the forecasting methodology for critical conditions of a dust storm affecting the southwest U.S. including the Fallon area.

APPROACH

The major components of the project were: (1) maintenance and data collection, quality control, and analysis of data from four special weather stations in the Fallon Naval Air Station area; (2) A case study of the dust storm in the southwestern U.S., completed using observations and modeling; and (3) use of categorical verification to evaluate the regional/mesoscale multi-model (COAMPS^{TM}, WRF, and MM5) ensemble forecasting system. The ensemble members for MM5 and WRF are generated by selecting different choices of physical parameterizations (planetary boundary layer (PBL) schemes, cumulus convection schemes, explicit cloud microphysical schemes, and radiation schemes) of each model, and perturbations of initial and boundary conditions (IC/BCs). Ensemble experiments were conducted on a 36 km grid (Fig. 1) nested into a 108 km grid that covers the entire North American continent and adjoining Pacific Ocean. The main objective is to obtain meaningful probability density functions (pdfs) for medium-to-long-range forecasting (from a week to 2 weeks) of the forecast variables; that is, to create and analyze pdfs for variables from each model and then combine the models (a three-model ensemble) with a total of 150 ensemble members generated from altering the physics options. An additional ensemble set of 100 WRF members was generated through perturbations of initial/lateral boundary conditions. The categorical verification measures employed in this study follow a contingency table of dichotomous events (Wilks 2006). In order to map continuous forecast outcomes (e.g., temperature) into a dichotomous event, we propose the following transformation. The events are considered using the statistical means (μ) and standard deviations (σ) of observed quantities for the entire simulation period at each of the radiosonde sites. The individual elements of the contingency table represent a number of events or occurrences for which the predicted variables *viz.,* air temperature, geopotential height, and winds, fall within or outside of an interval defined by observed means and standard deviations of observed quantities. This is illustrated in Figure 1.

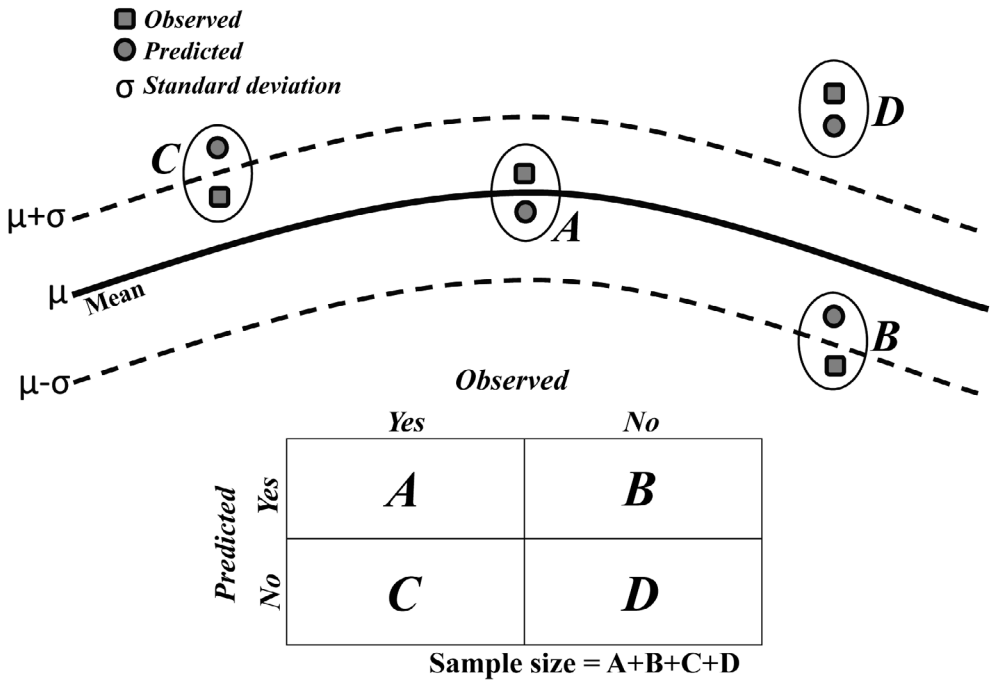

Figure 1. Schematic for categorical verification showing transformation of continuous forecast outcomes into dichotomous events.

The number of hits *A* defines the correct forecasts, and the correct negatives (*D*) provide the definition where neither the model predicted the event nor was the event observed. The elements *B* and *C* of the contingency table define the false alarms in the modeled events and the observed events missed in the model predictions, respectively. Both non-probabilistic and probabilistic verification scores are evaluated using the elements of the contingency table and forecast probabilities. Two scores that were calculated from the contingency tables and discussed here are the Bias (BIAS) and the Threat Score (TS). They are defined as follows:

$$BIAS = \frac{A+B}{A+C}$$

and

$$TS = \frac{A}{A+B+C}$$

where *n* is the total:

$$n = A+B+C+D$$

BIAS is a ratio of the frequency of predicted to observed events. A BIAS score of smaller (greater) than unity indicates that the events were under-estimated (over-estimated). A perfect forecast yields BIAS and TS scores to unity. The Brier score (*BS*) is a probabilistic verification metric based on forecast probabilities of dichotomous (binary) events. This gives the measure of the average square error of a probability forecast. This is analogous to the mean square error of a deterministic forecast, but the forecasts are given in probabilities. The Brier score (BS) is given as follows:

$$BS = \frac{1}{n}\sum_{k=1}^{n}\left(F_k - O_k\right)^2$$

where n is the number of points in the spatio-temporal domain. F_k is the probability of successful forecast occurrence from all the members of the ensemble at each station. In this study $n = 23$ (the total number of radiosonde locations used in the analysis). The probability of detection [$POD = A/(A+C)$] at each station is used for forecast probabilities. *POD* describes the likelihood of an event having been forecasted given that it has occurred. The binary event O_k is described as follows:

$$O_k = \begin{cases} 1, & \text{event occurs} \\ 0, & \text{event does not occur} \end{cases}$$

The definition of the event is the same as used in non-probabilistic verification. The range of BS varies from 0 to 1, and a perfect forecast yields a score of zero; and

(4) A new method has been developed to produce perturbations of boundary conditions. The method applies an error growth ratio into the perturbation of boundary conditions, so that the perturbation is changing with time.

If there is a small error in the initial conditions, the error gets greater as the forecast range gets longer and then reaches the saturated value (Lorenz 1982). A random perturbation (RP) is taken as the assumed initial error, and the perturbation for the later times increases in the ratio (Jiang et al. 2010)

$$RP_{LBCs}(t) = RP_0 * \frac{E(t)}{E_0} \qquad (3)$$

Based on the random perturbation, the perturbation is transformed to model space via the control variable transform (Barker et al 2003, 2004):

$$x' = URP_{LBcs} = U_p U_v U_h RP_{LBcs} \qquad (4)$$

The expansion $U=U_p\ U_v\ U_h$ represents the various stages of covariance modeling: horizontal correlations U_h, vertical covariances U_v, and multivariate covariances U_p. The perturbation for LBCs is varying with time with perturbation of temperature, U, V, and pressure, without perturbation of water vapor.

WORK COMPLETED

The skill of the multi-model ensemble forecast products was analyzed based on: (a) statistical verification to estimate the skill scores; (b) pdf diagnosis, statistics, and evolution; (c) rank histograms (Talagrand diagrams); and (d) evolution and spread of parameter trajectories ("spaghetti plots": Superposition of forecast isolines for the ensemble members).

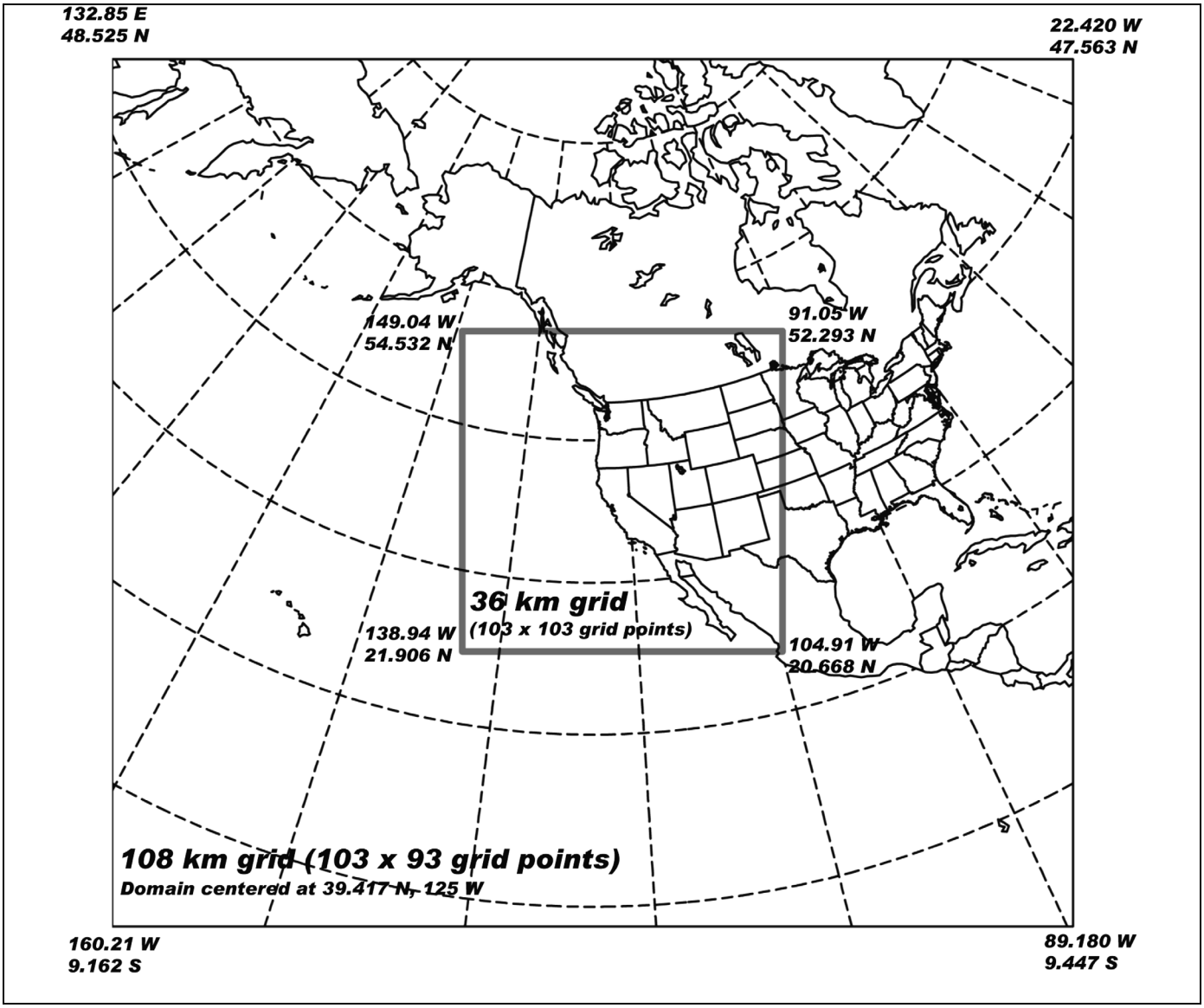

Figure 2. The WRF, MM5, and COAMPS model domains for the ensemble runs with 108 and 36 km on the coarse and nested grids, respectively.

The main ensemble technique was developed and updated for MM5, WRF, and COAMPS using a sufficient set of physics parameterization options that are available for a period of 15 days (12-27 December 2008). The physics options consisted of a variety of PBL schemes, single and double-moment cloud microphysics, simple to complex radiation, and cumulus parameterization schemes. The simulated case period was chosen because of the two intense frontal passages that occurred over NW Nevada. The initial and boundary conditions for MM5 and WRF were retrieved from the NCEP's Global Forecast System (GFS; http://www.emc.ncep.noaa.gov/). The Navy Operational Global Atmospheric Prediction System NOGAPS 4.0 (archived on 54 km grid; Bayler and Lewit 1992) forecast products were used as the initial analysis fields for COAMPS™ .

The source of numerical model uncertainty could be model physics, initial condition, and or lateral boundary conditions (Stensrud et al. 2000, Stensrud 2001, Stensrud et al. 2002, Baumhefner 1982). Meanwhile ensemble size is another factor for how much uncertainty could be expressed by an numerical model ensemble (Houtekamer et al. 1999). According to Baumhefner and Perkey 1982, errors in the data specified at the lateral boundary can propagate inward. A new experiment using perturbations of the lateral boundary conditions was completed with 50 ensemble members. The perturbed lateral boundary conditions were updated every 12 hours.

Table 1. Ensemble set of physical parameterizations and setup parameters for COAMPS.

No.	PBL	dxmeso*	Ice nucleation	Autoconversion factor
1	Mellor-Yamada (MY)	50000	Cooper and Haines (1986)	0.0004
2	Mellor-Yamada	10000	Cooper and Haines (1986)	0.0004
3	Mellor-Yamada	150000	Cooper and Haines (1986)	0.0004
4	Mellor-Yamada	150000	Cooper and Haines (1986)	0.0004
5	Mellor-Yamada	50000	Cooper and Haines (1986)	0.0004
6	Mellor-Yamada	10000	Cooper and Haines (1986)	0.0004
7	Mellor-Yamada	150000	Fletcher (1962)	0.0004
8	Mellor-Yamada	50000	Fletcher (1962)	0.0004
9	Mellor-Yamada	10000	Fletcher (1962)	0.0004
10	Mellor-Yamada	10000	Fletcher (1962)	0.001 default
11	Mellor-Yamada	50000	Fletcher (1962)	0.001 default
12	Mellor-Yamada	150000	Fletcher (1962)	0.001 default
13	Mellor-Yamada	50000	Cooper and Haines (1986)	0.001 default
14	Mellor-Yamada	10000	Cooper and Haines (1986)	0.001 default
15	Mellor-Yamada	150000	Cooper and Haines (1986)	0.001 default
16	Mellor-Yamada	150000	Cooper and Haines (1986)	0.001 default
17	Mellor-Yamada	50000	Cooper and Haines (1986)	0.001 default
18	Mellor-Yamada	10000	Cooper and Haines (1986)	0.001 default
19	Mellor-Yamada	10000	Cooper and Haines (1986)	0.002
20	Mellor-Yamada	50000	Cooper and Haines (1986)	0.002
21	Mellor-Yamada	150000	Cooper and Haines (1986)	0.002
22	Mellor-Yamada	150000	Cooper and Haines (1986)	0.002
23	Mellor-Yamada	50000	Cooper and Haines (1986)	0.002
24	Mellor-Yamada	10000	Cooper and Haines (1986)	0.002
25	Mellor-Yamada	10000	Fletcher (1962)	0.002
26	Mellor-Yamada	50000	Fletcher (1962)	0.002
27	Mellor-Yamada	150000	Fletcher (1962)	0.002
28	Modified MY version	10000	Cooper and Haines (1986)	0.0004
29	Modified MY version	50000	Cooper and Haines (1986)	0.0004
30	Modified MY version	150000	Cooper and Haines (1986)	0.0004
31	Modified MY version	150000	Cooper and Haines (1986)	0.0004
32	Modified MY version	50000	Cooper and Haines (1986)	0.0004
33	Modified MY version	10000	Cooper and Haines (1986)	0.0004
34	Modified MY version	10000	Fletcher (1962)	0.0004
35	Modified MY version	50000	Fletcher (1962)	0.0004
36	Modified MY version	150000	Fletcher (1962)	0.0004
37	Modified MY version	150000	Fletcher (1962)	0.001 default
38	Modified MY version	50000	Fletcher (1962)	0.001 default
39	Modified MY version	10000	Fletcher (1962)	0.001 default
40	Modified MY version	10000	Cooper and Haines (1986)	0.001 default
41	Modified MY version	50000	Cooper and Haines (1986)	0.001 default
42	Modified MY version	150000	Cooper and Haines (1986)	0.001 default
43	Modified MY version	150000	Cooper and Haines (1986)	0.001 default
44	Modified MY version	50000	Cooper and Haines (1986)	0.001 default
45	Modified MY version	10000	Cooper and Haines (1986)	0.001 default
46	Modified MY version	10000	Cooper and Haines (1986)	0.002
47	Modified MY version	50000	Cooper and Haines (1986)	0.002
48	Modified MY version	150000	Cooper and Haines (1986)	0.002
49	Modified MY version	150000	Cooper and Haines (1986)	0.002
51	Modified MY version	50000	Cooper and Haines (1986)	0.002
51	Modified MY version	10000	Cooper and Haines (1986)	0.002

Cumulus scheme = Kain-Fritsch parameterization (Kain and Fritsch 1993)
dxmeso=horizontal grid resolution (in m) below which cumulus scheme is turned off.*
Microphysics = Rutledge and Hobbs (1994) and Schmidt (2001)
Autoconversion factor used in the conversion of cloud water to drizzle/rain processes.
Radiation scheme follows Harshavardhan et al. (1987).
PBL scheme = Mellor-Yamada level 2.5 model (used in COAMPS 3) and modified version in COAMPS 4.

RESULTS

The results from the categorical verification using the Bias, Threat Score, and Brier Score for the temperature, geopotential height, and horizontal winds are shown in Figure 3.

Figure 3. Categorial verification scores of Bias (top row), Threat Score (middle row), and Brier Score (bottom row) for COAMPS (blue), MM5 (red), and WRF (green) from the 500 and 700 hPa ensemble forecasts for the temperature, geopotential height, and wind components valid at OAK (left column) and REV (right column).

The observed mean/standard deviation for temperature at 500 hPa (700 hPa) at OAK and REV are 250.2/6.6 K, and 248.1/6.8 K (265.0/5.9 K, and 263.5/5.2 K), respectively (Fig. 3). These values were taken as a basis for transformation into the events. Generally, the scores are similar for all models and there are no significant differences between the results for a coastal vs. inland station. Regarding the Bias, all models tend to underestimate the events, especially for the temperature and geopotential fields. This is mainly due to a greater number of missing events (C) in the models' forecasts at lower levels. Additional statistics of coastal vs. inland station data indicate that there are no significant

differences in POD as an effect of topographic complexity. All of the models showed Brier Scores less than 0.16. In this example, this is an empirical threshold value for all the models. The scores are similar at both levels. COAMPS shows some greater values, especially at the 500 hPa level, possibly due to the inaccuracies in the boundary conditions provided by NOGAPS. None of the models is superior at both levels and for all parameters, which confirms that the concept of a multi-model ensemble is valid and advantageous to use.

With perturbation of the lateral boundary conditions, the spread of the ensemble is comparable with the RMSE of the ensemble mean, while the spread of the ICs (initial conditions) ensemble was 1/3 smaller after the eight-day forecast time step. Our other study also shows that with a ten-member LBCs (Lower Boundary Conditions) ensemble, the RMSE of the ensemble mean got smaller than the control run (Jiang et al. 2011). Table 1 shows the RMSEs of the temperature, geopotential height, and U and V wind components. Compared to the physics ensemble, the RMSEs of the wind components at 700 mb and 925 mb from the LBCs ensemble are smaller; while those of geopotential height are smaller at 500 mb and 700 mb, and smaller at 500 mb for temperature. For wind components, at lower levels the LBCs ensemble shows smaller RMSE, however, for temperature and geopotential height it shows greater RMSE.

The time series of temperature and geopotential height (Figure 4) show that in the LBCs' ensemble there is a member that represented both the first and second fronts (member 38). Especially, the second front was missing in the ICs ensemble and the ensemble members with variations in physical parameterizations.

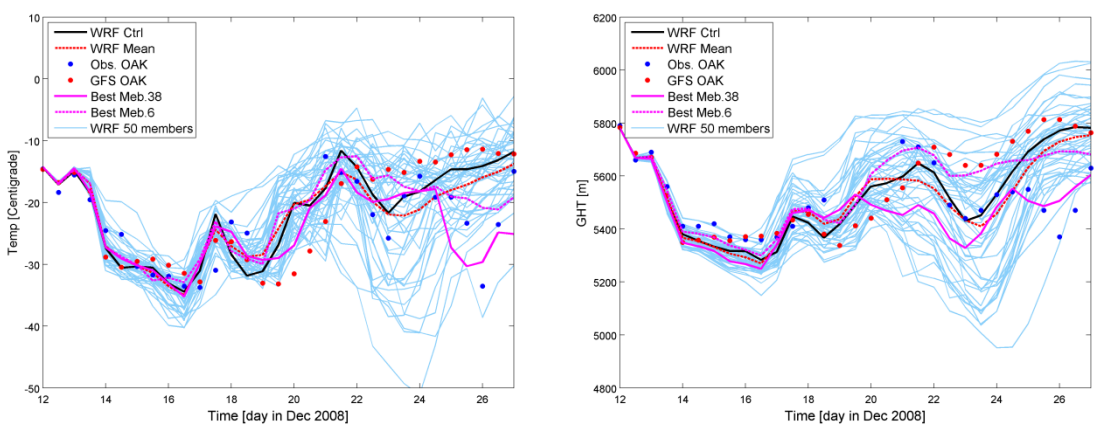

Figure 4. Temperature (right) and Geopotential height (left) at 500hPa at OAK, CA, from LBCs ensemble (without perturbation of water vapor). The "best" members are the ones showing the smallest RMSEs.

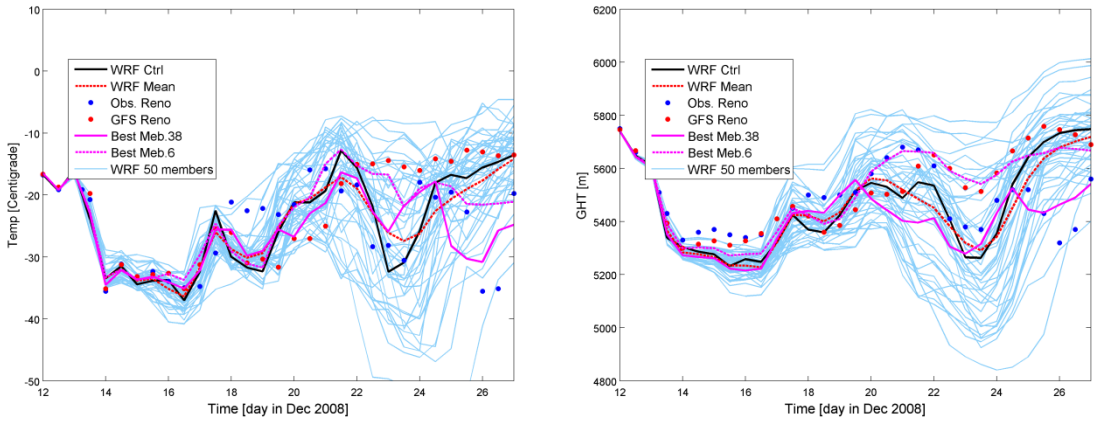

Figure 5. Same as Figure , but for Reno, NV.

Figures 4 and 5 also show the importance of accurate lateral boundary conditions. Note that GFS was not able to reproduce the front at the end of the period and consequently WRF was not able to predict the front. However, several of the ensemble members indicate possible low probability of the temperature drop at the end of the period, even though the lateral boundary conditions were not accurate. Because of the variations in RMSEs by parameters and levels, there is not an easy way to determine which ensemble member is better.

Table 1. RMSEs of temperature, geopotential height, U and V wind components at 500 mb, 700 mb, and 925 mb, from physics ensemble and LBCs ensemble, against radiosonde observations.

Variable	level	Phys. ensemble	LBCs ensemble
Temperature	500	5.778	5.667
	700	5.679	6.402
	925	4.3712	6.285
Geopotential height	500	143.433	131.944
	700	98.343	92.200
	925	78.51	97.118
U-wind	500	9.722	11.040
	700	9.388	8.223
	925	7.943	6.732
V-wind	500	14.558	15.106
	700	11.748	9.133
	925	7.091	6.928

In order to gain insight into the behavior of the models and the effects of the various physical parameterizations, we examined the WRF outputs differences in which only one physical parameterization was varied while other three were kept constant. That can tell us the extent to which particular parameterizations affect simulation results and differences. Figure 6 shows the effects on temperature at Reno and Oakland when three PBL schemes were changed while the other options were kept constant.

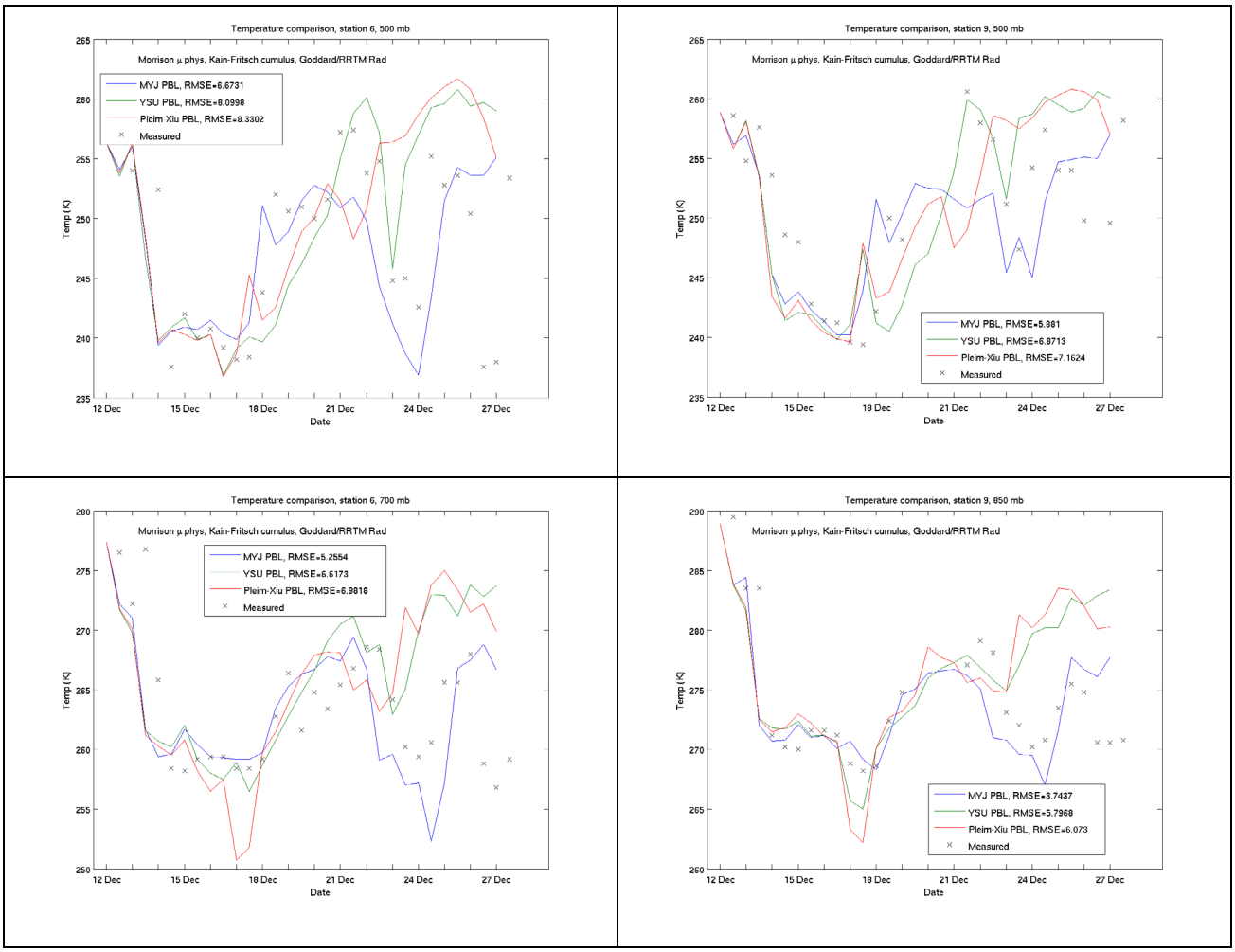

Figure 6. Effects of varying PBL schemes on the evolution of the temperature. Left column is Reno (KREV; 500 and 700 hPa), right column is Oakland (KOAK; 500 and 850 hPa). The root mean square errors are labeled in the legend.

Note that the most of differences occur for the frontal passages and that the YSU and Pleim-Xiu schemes show more similarities compared to the MYJ scheme. The temperature differences reach 20 degrees or more, especially during the passages. The MYJ scheme tends to produce large differences compared to other two schemes. The behavior of the temperature evolution at lower levels is more similar than aloft. With comparison against radiosonde observation, the RMSEs from the MYJ scheme are 1 to 2 K smaller than those from the YSU or Pleim-Xiu schemes.

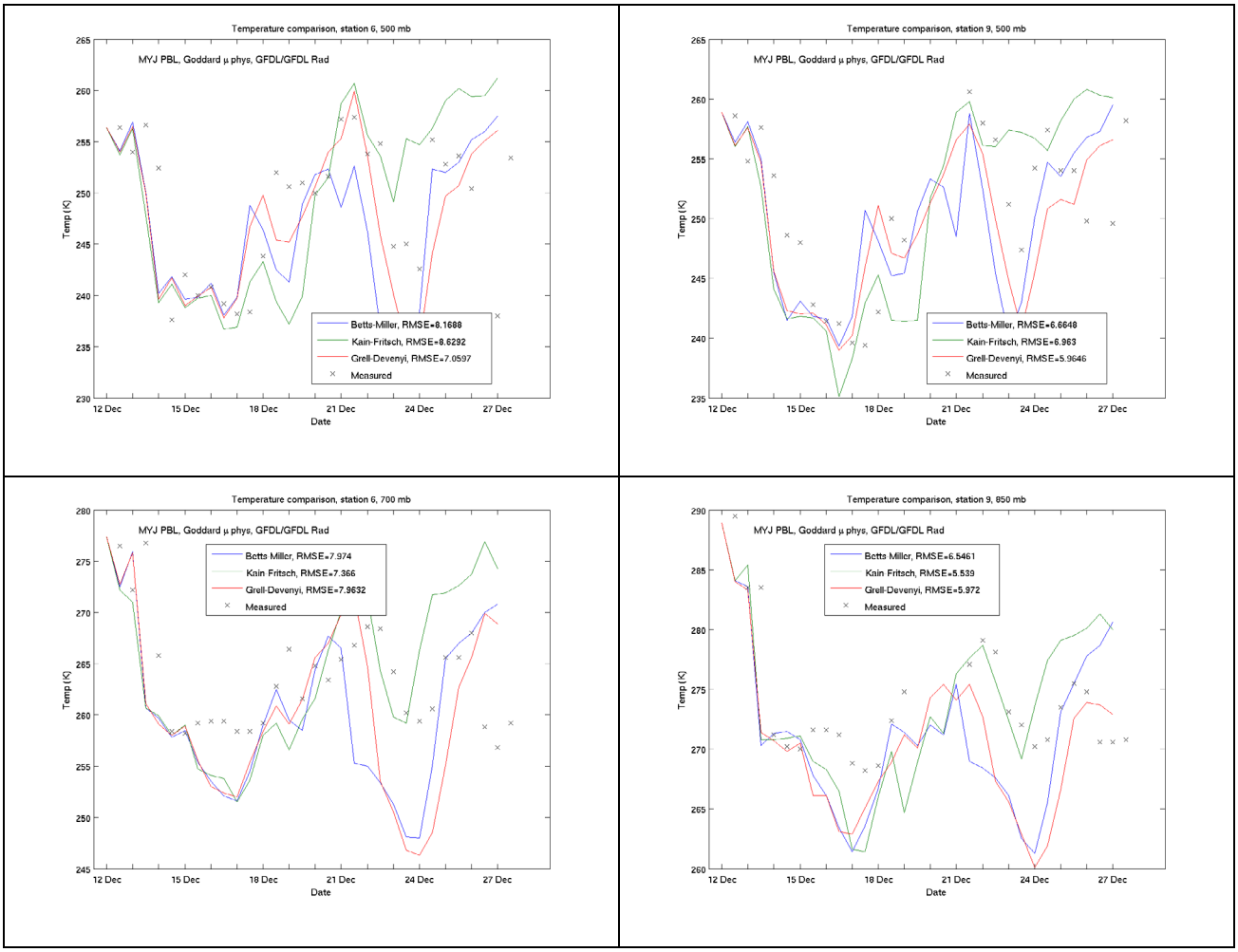

Figure 7. Effects of varying radiation schemes on the evolution of the temperature. Left column is Reno (KREV; 500 and 700 hPa), right column is Oakland (KOAK; 500 and 850 hPa). The root mean square errors are labeled in the legend.

Although there are some differences in the temperature time series, it is obvious that the variations of the radiation schemes have a secondary effect compared to PBL scheme variation on the temperature evolution. All three radiation schemes show a similar effect on the temperature at both locations and all levels. Maximum differences are generally less than 10 degrees. According to the RMSEs, at 500 mb the RMSEs from Grell-Devenyi scheme are smallest, while on 700 mb and 850mb, the RMSEs from Kain-Fritsch scheme are smallest.

IMPACT/APPLICATIONS

Although ensemble forecasting has been used for global predictions at major forecasting centers, regional and mesoscale ensemble forecasting is currently in the research and development stage. Furthermore, high-resolution multi-model ensemble forecasting holds promise for regional/mesoscale models' structure through exploration of physical parameterizations that are necessary to improve high-resolution forecasts in complex terrain. Although our research is progressing, the currently available

real time forecasts are accessible by the Fallon Naval Air Station and will hopefully improve operational nowcasts and forecasts crucial to the Navy's operations.

TRANSITIONS

Both the special set of four weather stations in the Fallon area [http://www.wrcc.dri.edu/] and the ongoing WRF operational forecasting system [http://www.adim.dri.edu/] have been developed as a complement to the forecasting and nowcasting at the Navy's Fallon Naval Air Station. The study will also provide guidance for future generations of multi-model ensemble forecasting for the Navy's operations. In particular, the results provide valuable information regarding the future use of the COAMPS model for probabilistic forecasts.

RELATED PROJECTS

Dr. Koracin is a co-P.I. on an ARO Project entitled "Forecasting of Desert Terrain" where real-time experience and expertise is facilitating an interdisciplinary project linking dust emission modeling (McAlpine et al., 2010), mesoscale atmospheric predictions (MM5 and WRF) (Zabkar et al. 2010), Lagrangian Stochastic Random Particle Dispersion modeling (Koracin et al. 2011, Chen et al. 2010, Lowenthal et al. 2010), and Computational Fluid Mechanics simulations. Dr. Koracin is a Lead Investigator for a Climate Modeling component of the multi-institutional NSF-EPSCoR Project on Climate Change, where they are developing new methods of weather and climate forecasting and use of satellite data assimilation for model evaluation (Jiang et al, 2011a). He is a task leader on another NSF EPSCoR project for the development of the Cyber-infrastructure and workforce activities. They are also investigating predictability limitations and chaotic behavior in weather and climate predictions and methods of downscaling global model results to regional, mesoscale, and microscale applications (Jiang et al, 2010 & 2011b). As a Principal Investigator on a DOE-NREL Wind Energy project, he is improving high-resolution forecasts in complex terrain (Jiang et al, 2011b). Dr. Koracin is a Principal Investigator on a DOE-Office of Science project, Simulating Climate on Regional Scale: North Pacific Mesoscale Coupled Air-Ocean Simulations Compared with Observations. The main task is to fully couple the ocean model (POP) and the atmospheric model (WRF) over the open ocean and coastal regions and estimate current and future projections of the Kuroshio Current effects on Pacific climate.

Dr. Lewis is involved in two projects that complement this ensemble research; (1) a variational analysis used to identify sources of error in dynamical prediction, and (2) analysis and prediction of dust storms over the western U.S. Both projects are supported by NOAA and this ONR project.

REFERENCES

Barker, D.M., W. Huang, Y. R. Guo, and Q. N. Xiao., 2004: A Three-Dimensional (3DVAR)Data Assimilation System For Use With MM5: Implementation and Initial Results. Mon. Wea. Rev., 132, 897-914.

Baumhefner, D. P. and D. J. Perkey. Evaluation of lateral boundary errors in a limited-domain model. *Tellus*, 1982, 34, 409-428.

Bayler, G. and H. Lewit , 1992: The Navy Operational Global and Regional Atmospheric Prediction System at the Fleet Numerical Oceanography Center. *Weather and Forecasting*, **Vol. 7**, No. 2.

Casati, B., and Coauthors, 2008: Forecast verification: Current status and future directions. *Meteor. Appl.,* **15**, 3–18.

Grell, G.A., J. Dudhia and D.R. Stauffer, 1994: *A Description of the Fifth-Generation Penn State/NCAR Mesoscale Model (MM5).* National Center for Atmospheric Research, Techn. Note TN-398, 122 pp.

Hodur, R. M., 1997: The Naval Research Laboratory's Coupled Ocean/Atmosphere Mesoscale Prediction System (COAMPS). *Mon. Wea. Rev*., **125**, 1414-1430.

Hou D., E. Kalnay, and K. K. Drogemeier, 2001. Objective Verification of the SAMEX'98 Ensemble Forecast. *Monthly Weather Review*, **129**:73-91.

Houtekamer, P. L., and H. L. Mitchell, 1999: Reply. *Mon. Wea. Rev*., **127**, 1378-1379.

Lorenz, E. N., 1982: Atmospheric predictability experiments with a large numerical model. *Tellus*, **34**, 505-513.

Skamarock, W.C., and Coauthors, 2008: *A description of the Advanced Research WRF Version 3,* NCAR Tech. Note. TN-475+STR, 113 pp. [Available from:

http://www.wrf-model.org/wrfadmin/docs/arw_v2.pdf].

Stensrud, D. J., 2001: Using short-range ensemble forecasts for predicting severe weather events. *Atmos. Res.*, **56**, 3-17.

Stensrud, D. J., and S. J. Weiss, 2002: Mesoscale model forecasts of the 3 May 1999 tornado outbreak. *Wea. Forecasting*, **17**, 526-543.

Stensrud, D. J., J.-W. Bao, and T. T. Warner, 2000: Using initial condition and model physics perturbations in short-range ensemble simulations of mesoscale convective systems. *Mon. Wea. Rev*., **128**, 2077-2107.

Wilks, D. S., 1995: Statistical Methods in the Atmospheric Sciences—An Introduction. International Geophysics Series, Vol. 59, Academic Press, 467 pp.

Wilks, D. S., 2006: Statistical Methods in the Atmospheric Sciences. 2d ed. International Geophysics Series, Vol. 91, Academic Press, 627 pp

PUBLICATIONS

Bebis, G., R. Boyle, B. Parvin, D. Koracin, R. Chung, R. Hammound, M. Hussain, T. Kar-Han, R. Crawfis and D.Thalmann, 2010: Advances in Visual Computing. *Lecture Notes in Computer Science*, **6455**, 2010, Springer Publishing. DOI: 10.1007/978-3-642-17277-9.

Chen, L.-W.A., D. Lowenthal, J.G. Watson, D. Koracin, D. Dubois, R. Vellore, N. Kumar, E.M. Knipping, N. Wheeler, K. Craig, S. Reid, 2010: Factors or sources: investigation of multivariate receptor modeling with simulated PM2.5 data. *J. Air & Waste Manage. Assoc.*, **60**, 43-54.

Jiang J., D. Koracin, R. Vellore, M. Xiao, J. M. Lewis, 2010: Using initial and boundary condition perturbations in medium-range regional ensemble forecasting with two nested domains. AGU 2010. San Francisco, California, U.S.A. 13-17 December 2010.

Jiang J., D. Koracin, R. Vellore, K. Horvath, R. Belu, 2011a: Application of variational data assimilation to dynamical downscaling of regional wind energy resources in the western U.S. Third International Conference on Computational Methods in Engineering and Science. May 9-13, 2011, South Lake Tahoe, U.S.A. (presentation)

Jiang J., D. Koracin, R. Vellore, K. Horvath, R. Belu, T. McCord, 2011b: Ensemble forecasting and uncertainty in wind and wind power prediction. EGU 2011. 03-08 April 2011, Vienna, Austria.

Jiang J., D. Koracin, R. Vellore, M. Xiao, J. M. Lewis, 2010: Using initial and boundary condition perturbations in medium-range regional ensemble forecasting with two nested domains. AGU 2010. San Francisco, California, U.S.A. 13-17 December 2010.

Kaplan, M., R. Vellore, and J. Lewis, 2011: Dust storm over the Black Rock Desert: Subsynoptic analysis of unbalanced circulations across the jet streak. Submitted November, 2010, Accepted July 2011.

Koracin, D., R. Vellore, D. H. Lowenthal, J. G. Watson, J. Koracin, T. McCord, D. W. DuBois, L.-W. Antony Chen, N. Kumar, E. M. Knipping, N. J. M. Wheeler, K. Craig, and S. Reid. 2011: Regional source identification using Lagrangian stochastic particle dispersion and HYSPLIT backward-trajectory models. *J. Air & Waste Manage. Assoc.*, **61**, 660-672. DOI:10.3155/1047-3289.61.6.660.

Lewis, J. M., M. L. Kaplan, R. Vellore, R. M. Rabin, J. Hallett, and S. A. Cohn, 2011: Dust storm over the Black Rock Desert: Larger-scale dynamic signatures. *J. Geophys. Res. (Atmospheres)*, **116**, D06113, doi:10.1029/2010JD014784

Lowenthal, D. H., J. G. Watson, D. Koracin, L.-W. A. Chen, D. Dubois, R. Vellore, N. Kumar, E. M. Knipping, N. Wheeler, K. Craig, and S. Reid, 2010: Evaluation of regional scale receptor modeling. *J. Air & Waste Manage. Assoc.*, **60**, 26-42.

McAlpine, J.D., D. Koracin, D. P. Boyle, J. A. Gillies, and E. V. McDonald, 2010: Development of a rotorcraft dust-emission parameterization using a CFD model. *Environ. Fluid Mechan.*, **10**, 691-710.

Zabkar, R., J. Rakovec, and D. Koracin, 2010: The roles of regional accumulation and advection of ozone during high ozone episodes in Slovenia: a WRF/Chem modelling study. *Atmos. Environ*., **45**, 1192-1202.